

# Can microlensing fold caustics reveal a second stellar limb-darkening coefficient?

M. Dominik

*University of St Andrews, School of Physics & Astronomy, North Haugh, St Andrews, KY16 9SS*

18 June 2018

## ABSTRACT

Dense high-precision photometry of microlensed stars during a fold-caustic passage can be used to reveal their brightness profiles from which the temperature of the stellar atmosphere as function of fractional radius can be derived. While the capabilities of current microlensing follow-up campaigns such as PLANET allowed for several precise measurements of linear limb-darkening coefficients, all attempts to reveal a second limb-darkening coefficient from such events have failed. It is shown that the residual signal of a second coefficient characterizing square-root limb darkening is  $\sim 25$  times smaller which prevents a proper determination except for unlikely cases of very high caustic-peak-to-outside magnification ratios with no adequate event being observed so far or for source stars passing over a cusp singularity. Although the presence of limb darkening can be well established from the data, a reliable measurement of the index of an underlying power-law cannot be obtained.

**Key words:** gravitational lensing – stars: atmospheres.

## 1 INTRODUCTION

Since Schneider & Weiß (1987) have proposed to use caustics of gravitational lenses for measuring the brightness profile of closely-aligned background sources, dense high-precision photometry on microlensing events involving fold-caustic passages has provided measurements of linear limb-darkening coefficients for several stars (Albrow et al. 2000, 2001; Afonso et al. 2000; Fields et al. 2003).

For stellar brightness profiles that involve linear, square, or square-root terms in  $\cos \vartheta$ , where  $\vartheta$  is the emergent angle, properties of light curves during fold-caustic passages have been studied by Rhie & Bennett (1999), while prospects and strategies for determining the linear limb-darkening coefficient have recently been discussed in detail by Dominik (2004), showing the ability of obtaining precise measurements even with moderate use of the current capabilities.

This letter will however show that the measurement of additional coefficients, e.g. corresponding to a square-root law term, is not possible for typical events that involve a fold-caustic passage. Attempts of such measurements (Fields et al. 2003) have resulted in the meaningful measurement of a single linear combination of the involved limb-darkening coefficients only, while a similar result has been obtained for an event where the source passes over a cusp (Abe et al. 2003), where however the exhibited differential magnification is modest due to the source size being relatively large compared to the cusp. In contrast, the cusp-passage event discussed by Albrow et al. (1999a) provides a better size ratio between source and cusp and to date presents the only measurement of both linear and square-root limb-darkening coefficients by microlensing.

## 2 INTENSITY PROFILE AND LIGHTCURVE

With  $\bar{I}$  denoting the average brightness and  $\rho$  the fractional radius of an observed source star, its brightness profile for a given filter reads

$$I(\rho) = \bar{I} \xi(\rho), \quad (1)$$

where  $\xi(\rho)$  is a dimensionless function fulfilling the normalization

$$\int_0^1 \xi(\rho) \rho \, d\rho = \frac{1}{2}. \quad (2)$$

Let us consider the source passing a fold caustic during the time-span  $2 t_{\star}^{\pm}$  and let  $F_{\text{f}}^{\star}$  denote its flux at the beginning of a caustic entry or the end of a caustic exit at time  $t_{\text{f}}^{\star}$ . In the vicinity of the caustic, the observed flux can be approximated as (e.g. Albrow et al. 1999b; Dominik 2003)

$$F(t) = F_{\text{r}} \left( \frac{\hat{t}}{t_{\star}^{\pm}} \right)^{1/2} G_{\text{f}}^{\star} \left( \pm \frac{t - t_{\text{f}}^{\star}}{t_{\star}^{\pm}}; \xi \right) + F_{\text{f}}^{\star}, \quad (3)$$

where upper (lower) signs correspond to caustic entries (exits),  $F_{\text{r}}$  denotes a characteristic rise flux,  $\hat{t}$  is an arbitrarily chosen unit time, and the variation of images of the source that do not become critical as the caustic is approached is neglected. The caustic profile function  $G_{\text{f}}^{\star}(\eta; \xi)$  depends on the caustic passage phase  $\eta = \pm (t - t_{\text{f}}^{\star})/t_{\star}^{\pm}$  and is characteristic for the adopted stellar brightness profile  $\xi(\rho)$ , where (Heyrovský 2003)

$$G_{\text{f}}^{\star}(\eta; \xi) = \int_0^1 \mathcal{T}(\eta, \rho) \xi(\rho) \, d\rho, \quad (4)$$

and

$$\mathcal{T}(\eta, \rho) = 2\rho^{1/2} j\left(\frac{\eta-1}{\rho}\right). \quad (5)$$

With  $K$  denoting the complete elliptical integral of first kind,  $j(z)$  reads (Gaudi & Gould 1999)

$$j(z) = \begin{cases} 0 & \text{for } z \leq -1 \\ \frac{\sqrt{2}}{\pi} K\left(\sqrt{\frac{1+z}{2}}\right) & \text{for } -1 < z < 1 \\ \frac{2}{\pi\sqrt{1+z}} K\left(\sqrt{\frac{2}{1+z}}\right) & \text{for } z > 1 \end{cases}. \quad (6)$$

### 3 POWER-LAW PROFILES

A popular class of models for the stellar brightness profile  $\xi(\rho)$  is a linear superposition of terms proportional to powers of  $\cos\vartheta = \sqrt{1-\rho^2}$ , where  $\vartheta$  denotes the angle between the normal to the stellar surface and the direction to the observer. With the term proportional to  $\cos^p\vartheta$  reading

$$\xi_{\{p\}}(\rho) = (1+p/2)(1-\rho^2)^{p/2}, \quad (7)$$

the stellar brightness profile becomes

$$\xi(\rho; \Gamma_{\{p_1\}} \dots \Gamma_{\{p_k\}}) = 1 + \sum_{i=1}^k \Gamma_{\{p_i\}} [\xi_{\{p_i\}}(\rho) - 1] \quad (8)$$

with  $k$  coefficients  $0 \leq \Gamma_{\{p_i\}} \leq 1$  corresponding to the power  $p_i > 0$  which moreover are required to fulfill the condition

$$\sum_{i=1}^k \Gamma_{\{p_i\}} \leq 1. \quad (9)$$

According to Eq. (4), the caustic profile function  $G_f^*(\eta; \xi)$  inherits the linearity in  $\Gamma_{\{p_i\}}$  from  $\xi(\rho)$ , making it a superposition

$$G_f^*(\eta; \Gamma_{\{p_1\}} \dots \Gamma_{\{p_k\}}) = 1 + \sum_{i=1}^k \Gamma_{\{p_i\}} [G_{f,\{p_i\}}^*(\eta) - 1] \quad (10)$$

of the caustic profiles functions  $G_{f,\{p_i\}}^*(\eta) \equiv G_f^*(\eta; \xi_{\{p_i\}})$  which correspond to the stellar brightness profiles  $\xi_{\{p_i\}}(\rho)$ , where

$$G_{f,\{p\}}^*(\eta) = \frac{1}{\sqrt{\pi}} \frac{(1+\frac{p}{2})!}{(\frac{1+p}{2})!} \int_{\max(1-\eta, -1)}^{\max(1-\eta, 1)} \frac{(1-x^2)^{\frac{1+p}{2}}}{\sqrt{x+\eta-1}} dx. \quad (11)$$

### 4 MEASUREMENT OF SECOND COEFFICIENT

The stellar brightness profiles corresponding to uniform brightness ( $p=0$ ), linear limb darkening ( $p=1$ ) and square-root limb darkening ( $p=1/2$ ) are shown in Fig. 1, while the corresponding caustic profile functions are shown in Fig. 2. It can be seen that square-root limb darkening mediates between linear limb darkening and uniform brightness.

Let us compare maximal square-root limb darkening corresponding to the caustic profile function  $G_{f,\{1/2\}}^*(\eta)$  with its best approximation by a combination of uniform brightness and linear limb darkening

$$G_f^*(\eta; \Gamma) = (1-\Gamma) G_{f,\{0\}}^*(\eta) + \Gamma G_{f,\{1\}}^*(\eta) \quad (12)$$

which depends on the choice of a norm on the function space. By requiring

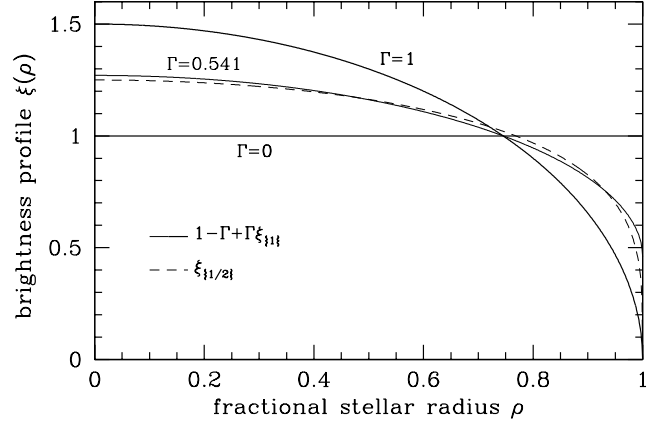


**Figure 1.** Stellar brightness profiles  $\xi(\rho)$  corresponding to different linear superpositions of power-law models. The solid lines refer to profiles  $\xi(\rho; \Gamma) = 1 - \Gamma + \Gamma \xi_{\{1\}}(\rho)$  which are affine-linear in  $\cos\vartheta$ , where  $\Gamma = 0$  corresponds to uniform brightness,  $\Gamma = 1$  to maximal linear limb darkening, and  $\Gamma = 0.541$  to the best approximation in the sense of Eq. (13) to maximal square-root limb darkening whose profile  $\xi_{\{1/2\}}(\rho)$  is shown as dashed line.

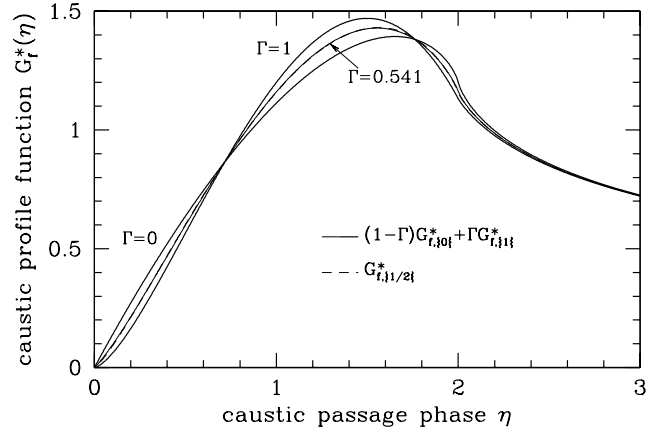


**Figure 2.** Caustic profile functions  $G_f^*(\eta; \xi)$  that correspond to the stellar brightness profiles shown in Fig. 1, where  $G_f^*(\eta; \Gamma) = (1-\Gamma) G_{f,\{0\}}^*(\eta) + \Gamma G_{f,\{1\}}^*(\eta)$  are plotted as solid lines for  $\Gamma = 0$  (uniform brightness),  $\Gamma = 1$  (maximal linear limb darkening), and  $\Gamma = 0.541$  (best approximation to maximal square-root limb darkening), while the caustic profile function  $G_{f,\{1/2\}}^*(\eta)$  for maximal square-root limb darkening is shown as dashed line.

$$\int_0^\infty [G_f^*(\eta; \Gamma) - G_{f,\{1/2\}}^*(\eta)]^2 d\eta \quad (13)$$

to adopt a minimum, the approximation is in maximal accordance with the use of  $\chi^2$  for sampled lightcurves and yields  $\Gamma = 0.541$  as optimal value. Figs. 1 and 2 also show the stellar brightness profile  $\xi(\eta; \Gamma)$  and the caustic profile function  $G_f^*(\eta; \Gamma)$ , respectively, that corresponds to this value. Since the caustic probes a combination of several fractional radii  $\rho$  for any caustic passage phase  $\eta$  which is characterized by  $\mathcal{T}(\eta, \rho)$  according to Eq. (4), significant differences between the brightness profiles are washed out in the corresponding caustic profile functions making the latter hardly distinguishable.

Let us assume that the uncertainties  $\sigma$  of the flux measurements  $F$  follow Poisson statistics, so that  $\sigma = \sigma_f^* (F/F_f^*)^{1/2}$ ,

where  $\sigma_f^*$  denotes the uncertainty for the flux  $F_f^*$  observed for the source being just outside the caustic. The ratio  $Z(\eta)$  between signal-to-noise for flux deviations  $\Delta F$  due to the different profiles and signal-to-noise for the flux  $F_f^*$  is then given by

$$\begin{aligned} Z_{\{1/2\}}(\eta) &= \frac{\Delta F(\eta)/\sigma}{F_f^*/\sigma_f^*} \\ &= \alpha_{\{1/2\}} \frac{G_f^*(\eta; \Gamma) - G_{f,\{1/2\}}^*(\eta)}{\sqrt{\alpha_{\{1/2\}} G_{f,\{1/2\}}^*(\eta) + 1}}, \end{aligned} \quad (14)$$

where

$$\alpha_{\{1/2\}} = \frac{(F_{\text{peak}}/F_f^*) - 1}{G_{\text{peak},\{1/2\}}} \quad (15)$$

with  $F_{\text{peak}}$  denoting the flux at the caustic peak corresponding to the maximum of  $G_{f,\{1/2\}}^*(\eta)$ , which is  $G_{\text{peak},\{1/2\}} \approx 1.431$ . For selected values of  $F_{\text{peak}}/F_f^*$ ,  $Z_{\{1/2\}}(\eta)$  is displayed in Fig. 3, where the linear limb-darkening coefficient has been optimized so that either the integrated squared deviation or the single largest absolute deviation is minimized. In general, the optimal choice of  $\Gamma$  depends on the sampling, and with only parts of the caustic passage being sampled, the signal may further decrease, also affected by adopting best-fit values for  $t_f^\pm$  and  $t_\pm^\perp$  that differ from the true values. While a uniform sampling is better represented by the former choice for an optimal linear limb-darkening coefficient, the latter choice better reflects the case where the beginning of a caustic entry or the end of the caustic exit is preferentially sampled being the region that provides the largest amount of information about the square-root limb-darkening coefficient.

For all fold-caustic events observed so far, the caustic-peak-to-outside magnification ratio is  $F_{\text{peak}}/F_f^* \lesssim 8$ , so that the measurement of  $\Gamma_{\{1/2\}}$  with an absolute uncertainty of 0.1 from a single point requires a relative flux uncertainty outside the caustic  $\sigma_f^*/F_f^* \lesssim 0.2\%$  for typical events, where this limit roughly increases proportional to  $F_{\text{peak}}/F_f^*$ .

For comparison, Fig. 4 shows the relative signal-to-noise ratio  $Z(\eta)$  for the detection of linear limb darkening against uniform brightness, where

$$Z_{\{1\}}(\eta) = \alpha_{\{1\}} \frac{G_{f,\{0\}}^*(\eta) - G_{f,\{1\}}^*(\eta)}{\sqrt{\alpha_{\{1\}} G_{f,\{1\}}^*(\eta) + 1}} \quad (16)$$

and

$$\alpha_{\{1\}} = \frac{(F_{\text{peak}}/F_f^*) - 1}{G_{\text{peak},\{1\}}}, \quad (17)$$

with  $G_{\text{peak},\{1\}} \approx 1.470$  being the maximum of  $G_{f,\{1\}}^*(\eta)$ .

From a simulation of a caustic exit with  $F_{\text{peak}}/F_f^* = 12.5$  lasting 12 h and being sampled on average every 6 min with an accuracy  $\sigma_f^*/F_f^* = 1.5\%$  in accordance with the capabilities of the PLANET campaign (Dominik et al. 2002), Dominik (2004) found that a linear limb-darkening coefficient  $\Gamma_{\{1\}} = 0.5$  can be measured with a relative uncertainty of  $\sim 2.5\%$ . With the residual signal of an additional square-root limb-darkening coefficient being  $\sim 25$  times smaller, the absolute uncertainty in  $\Gamma_{\{1/2\}}$  would be about 0.3 and not allow a meaningful measurement. In order to achieve an uncertainty of 0.1 for  $\Gamma_{\{1/2\}}$  in an event with  $F_{\text{peak}}/F_f^* = 8$ , one would therefore require a relative uncertainty of the flux measurement outside the caustic of  $\sigma_f^*/F_f^* \sim 0.3\%$  and less at the peak. With systematic effects dominating the photometric error bars rather than the photon noise at this level, this appears not to be achievable. In addition to large caustic-peak-to-outside

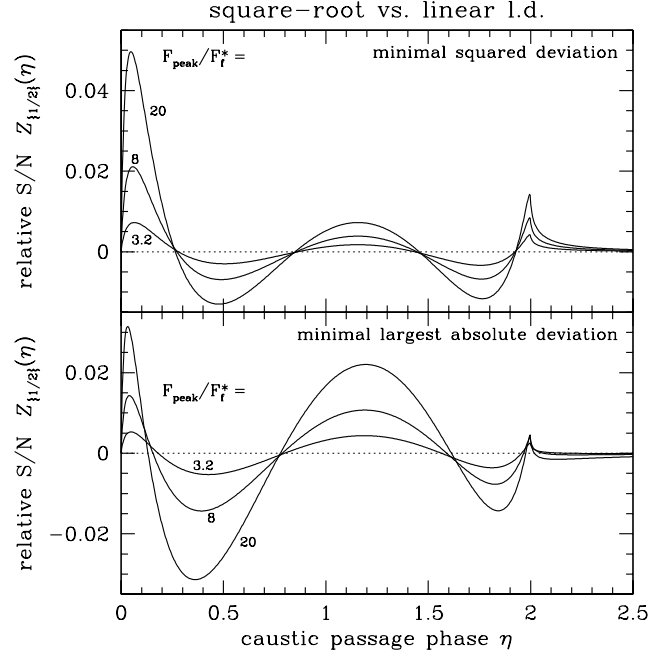


**Figure 3.** Ratio  $Z_{\{1/2\}}(\eta)$  between signal-to-noise  $\Delta F(\eta)/\sigma$  for the detection of maximal square-root limb darkening against the best-approximating affine-linear limb darkening and signal-to-noise  $F_f^*/\sigma_f^*$  for the flux measurement outside the caustic for selected caustic-peak-to-outside magnification ratios  $F_{\text{peak}}/F_f^*$ . In order to obtain the best approximation,  $\Gamma$  has been chosen so that the integrated square of  $Z_{\{1/2\}}(\eta) = (\Delta F(\eta)/\sigma)/(F_f^*/\sigma_f^*)$  is minimized for the curves shown in the upper panel, yielding  $\Gamma = 0.542, 0.544, \text{ or } 0.546$  for  $F_{\text{peak}}/F_f^* = 3.2, 8, \text{ or } 20$ , respectively, whereas the absolute maximum of  $Z_{\{1/2\}}(\eta)$  has been minimized for the curves shown in the lower panel yielding  $\Gamma = 0.567, 0.576, \text{ or } 0.586$  for the same values of  $F_{\text{peak}}/F_f^*$ .

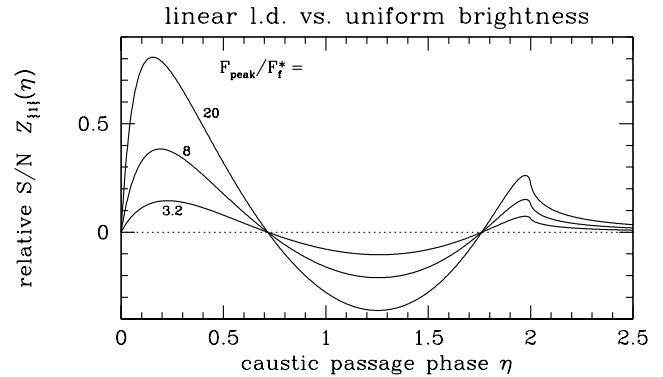


**Figure 4.** Ratio  $Z_{\{1\}}(\eta)$  between signal-to-noise  $\Delta F(\eta)/\sigma$  for the detection of maximal linear limb darkening against uniform brightness and signal-to-noise  $F_f^*/\sigma_f^*$  for the flux measurement outside the caustic for selected caustic-peak-to-outside magnification ratios  $F_{\text{peak}}/F_f^*$ .

magnification ratios  $F_{\text{peak}}/F_f^*$ , large fluxes  $F_f^*$  at the caustic outside also enhance the prospects for measuring limb-darkening coefficients by allowing better photometric accuracies  $\sigma_f^*/F_f^*$ .

## 5 MIXED LINEAR AND SQUARE-ROOT LAWS

With square-root limb darkening being fairly approximated by a superposition of linear limb-darkening and uniform brightness, pho-

ometric observations during the passage of a source star over a fold caustic appear to be blind to the power index of an adopted limb-darkening law.

Assuming the presence of both linear and square-root limb darkening, it is a linear combination of the corresponding limb-darkening coefficients that is probed in first instance.

Let us consider that maximal square-root limb darkening  $\xi_{\{1/2\}}(\rho)$  is best approximated by  $\xi(\rho; \gamma)$ , where  $\gamma$  depends on the data. The stellar brightness profile can then be written as

$$\xi(\rho) = 1 + \sum (\tilde{\Gamma}_{\pm} \tilde{\xi}_{\pm}(\rho) - 1), \quad (18)$$

where

$$\begin{aligned} \tilde{\xi}_{+}(\rho) &= \frac{1}{1+\gamma} [\xi_{\{1/2\}}(\rho) + \gamma \xi_{\{1\}}(\rho)], \\ \tilde{\xi}_{-}(\rho) &= \frac{1}{1-\gamma} [\xi_{\{1/2\}}(\rho) - \gamma \xi_{\{1\}}(\rho)] \end{aligned} \quad (19)$$

fulfill the normalization of Eq. (2) and analogous relations hold for  $G_f^*(\eta; \xi)$ . The mixed profiles  $\tilde{\xi}_{+}(\rho)$  and  $\tilde{\xi}_{-}(\rho)$  have been chosen so that  $\tilde{\xi}_{+}(\rho)$  combines best-matched equivalent profiles, whereas  $\tilde{\xi}_{-}(\rho)$  measures their difference. The corresponding limb-darkening coefficients are then given by

$$\begin{aligned} \tilde{\Gamma}_{+} &= \frac{1+\gamma}{2\gamma} [\gamma \Gamma_{\{1/2\}} + \Gamma_{\{1\}}], \\ \tilde{\Gamma}_{-} &= \frac{1-\gamma}{2\gamma} [\gamma \Gamma_{\{1/2\}} - \Gamma_{\{1\}}]. \end{aligned} \quad (20)$$

Therefore, the data will provide an accurate measurement of  $\tilde{\Gamma}_{+}$  similar to  $\Gamma = \Gamma_{\{1\}}$  if only linear limb darkening is considered (i.e.  $\Gamma_{\{1/2\}} = 0$ ), where one finds the correspondence  $\tilde{\Gamma}_{+} = [(1+\gamma)/(2\gamma)]\Gamma$  with  $\gamma \sim 0.54 \dots 0.60$ . With the influence of  $\xi_{-}(\rho)$  on the lightcurve being  $\sim 25$  times smaller than that of  $\xi_{+}(\rho)$ , the uncertainty in  $\tilde{\Gamma}_{-}$  corresponding to the second limb-darkening coefficient will exceed that in  $\tilde{\Gamma}_{+}$  by the same factor, and models that coincide in  $\tilde{\Gamma}_{\pm}$  are roughly equivalent.

With measurements of  $\tilde{\Gamma}_{+}$  and  $\tilde{\Gamma}_{-}$ , the coefficients corresponding to the linear and square-root term follow as

$$\begin{aligned} \Gamma_{\{1\}} &= \frac{\gamma}{1+\gamma} \tilde{\Gamma}_{+} - \frac{\gamma}{1-\gamma} \tilde{\Gamma}_{-}, \\ \Gamma_{\{1/2\}} &= \frac{1}{1+\gamma} \tilde{\Gamma}_{+} + \frac{1}{1-\gamma} \tilde{\Gamma}_{-}. \end{aligned} \quad (21)$$

## 6 SUMMARY AND FURTHER DISCUSSION

If the stellar brightness profile  $\xi(\rho)$  is modelled by a linear superposition of three base profile functions, as for the discussed examples of constant, linear, and square-root terms in  $\cos \vartheta$ , the normalization forces one of these profiles to mediate between the other two, so that this base profile can be approximated by a superposition of the others. With several fractional radii  $\rho$  being probed by the fold caustic for any passage phase  $\eta$  according to  $\mathcal{T}(\eta, \rho)$ , the residuals of this approximation are smaller for the caustic profile function  $G_f^*(\eta; \xi)$  than for the stellar brightness profile  $\xi(\rho)$ , which limits the power of photometric microlensing observations during fold-caustic passages for revealing the stellar brightness profile  $\xi(\rho)$ .

Compared to the determination of a linear limb-darkening coefficient, the residual signals of an additional square-root limb-darkening coefficient are  $\sim 25$  times smaller, making its measurement with current microlensing follow-up campaigns such as PLANET impossible, unless the caustic-peak-to-exit magnification ratio becomes  $F_{\text{peak}}/F_f^* \gtrsim 40$  for a (typical) photometric accuracy

$\sigma_f^*/F_f^* = 1.5\%$  at the caustic exit where none of such events have been observed so far, or the source passes over a cusp singularity rather than a fold.

If more than one limb-darkening base profile is assumed to contribute, only a single characteristic coefficient can be accurately measured which corresponds to a specific superposition of the corresponding base profiles as found for worked examples (Fields et al. 2003; Abe et al. 2003).

## ACKNOWLEDGMENTS

This work has been made possible by postdoctoral support on the PPARC rolling grant PPA/G/O/2001/00475. This letter provides the first part of the answer to a question asked by P.D. Sackett several years ago.

## REFERENCES

- Abe F., et al., 2003, A&A, 411, L493
- Afonso C., et al., 2000, ApJ, 532, 340
- Albrow M. D., et al., 1999a, ApJ, 522, 1011
- Albrow M. D., et al., 1999b, ApJ, 522, 1022
- Albrow M. D., et al., 2000, ApJ, 534, 894
- Albrow M. D., et al., 2001, ApJ, 549, 759
- Dominik M., 2003, Theory and practice of microlensing light-curves around fold singularities, astro-ph/0309581
- Dominik M., 2004, Revealing stellar brightness profiles by means of microlensing fold caustics, astro-ph/0402564
- Dominik M., et al., 2002, P&SS, 50, 299
- Fields D. L., et al., 2003, ApJ, 569, 1305
- Gaudi B. S., Gould A., 1999, ApJ, 513, 619
- Heyrovský D., 2003, ApJ, 594, 464
- Rhie S. H., Bennett D. P., 1999, Line Caustic Microlensing and Limb Darkening, astro-ph/9912050
- Schneider P., Weiß A., 1987, A&A, 171, 49